DESIRABILITY OF USING A FAST SAMPLING RATE FOR COMPUTING WIND VELOCITY FROM PILOT-BALLOON DATA

HENRY RACHELE and LOUIS D. DUNCAN

Atmospheric Sciences Laboratory, U.S. Army Electronics Command, White Sands Missile Range, N. Mex.

ABSTRACT

Advantages of using a fast sampling rate for providing raw data for computing wind velocities from pilot-balloon observations are discussed. Two independent approaches show that (for a given sampling rate) the errors in the mean wind computed through a layer tend to be smaller the larger the layer. However, if many observations are used to compute the mean wind through a layer, the computed wind is more accurate than that obtained by using just two observations, one at the bottom and one at the top of the layer. Graphs are presented which give relative estimates of wind errors as a function of sampling interval, sampling rate, and mean wind speed.

1. INTRODUCTION

In recent years, systems have been developed at White Sands Missile Range (WSMR) for collecting and processing pilot-balloon data in real time. One such system uses conventional manually operated balloon-tracking theodolites which have been modified for automatic readout. This allows the operators to track the balloon continuously and precludes the necessity of periodic stops for visual readings as with conventional methods. The angular data from the theodolites are continuously transmitted in analog form to a central point where they are digitized for processing by the computer. The system in general is discussed in two reports by Rachele and Duncan [2], [4].

The practice has been to use data digitized at the rate of one data frame per second (azimuth and elevation angles from each theodolite every second).

A question has arisen as to the merit of having data available at a fast rate, particularly in view of results published by Barnett and Clarkson [1], obtained from empirical data, which state that data taken at a rate less than one frame per 20 sec. is subject to progressively greater error the shorter the time increment between observations. Specifically, the following is summarized from their paper:

Five series of simultaneous observations from three theodolites were made to investigate the accuracy of double theodolite observations. The three theodolites A, B, C formed a triangle with two sides 1,000 m. long and the other 1,414 m. long. Five sequences of pilot balloon observations were made with the three theodolites on each of five different days. On each day one sequence was made with a 5-sec. interval between observations, one with a 10-sec. interval, one with a 20-sec. interval, one with a 30-sec. interval, and one with a 60-sec. interval. Azimuth and elevation angles were read to 1/10 of a degree.

The data were divided into three sets of double theodolite readings: theodolites A and B, B and C, and A and C. Simultaneous angles were used to calculate the horizontal projection of the mean balloon path between two successive observation times. This resulted in three wind vectors to represent the same wind condition experienced by the balloon between each two successive observation times.

For each set of three wind vectors, the magnitude of the smallest was divided by the magnitude of the largest to obtain the "horizontal wind speed accuracy ratio." A ratio of 100 percent is obtained only when all three vectors are of exactly the same magnitude. Likewise, the maximum difference in direction between any two was called the "horizontal wind direction error." In this case, a smaller number indicates greater accuracy.

To insure the validity of the results, observations for the first day were not used, the order in which the different observational time intervals were used was different each day, all sets of data for any one observation were discarded if any azimuth angle was within 5° of a base line to another theodolite, and data were discarded for wind speeds less than 3 m.p.h.

For each time interval, the means were found for the "horizontal wind speed accuracy ratio" and for the "horizontal wind direction error." The results are shown in figure 1.

The purpose of this report is to present an evaluation of theoretical results of using fast sampling rates (one per second) as in the real-time system.

2. DISCUSSION

In this evaluation, the following assumptions are made: (1) At least two theodolites are used. (2) There is no bias between the two theodolites, i.e., no orientation or leveling errors, and no differences in precision. (3) There is no

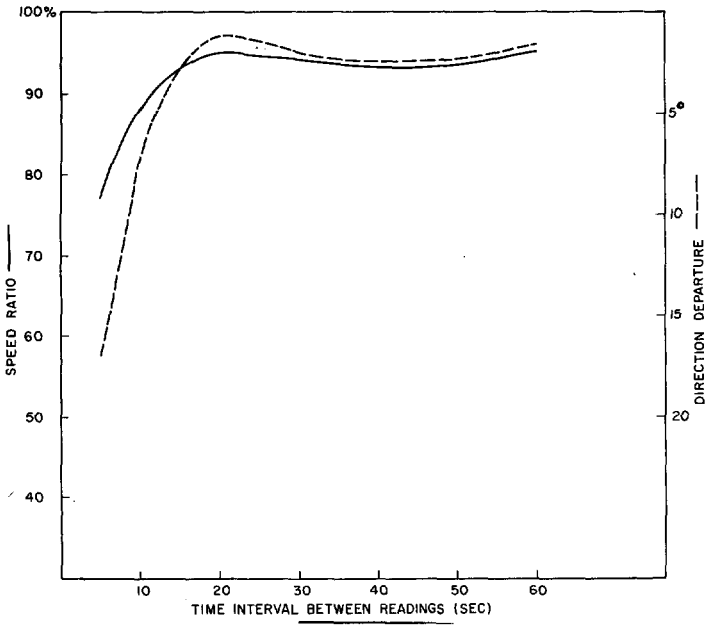

FIGURE 1.—Speed accuracy ratio, and wind direction error as functions of time interval between observation readings. Graph by Barnett and Clarkson [1].

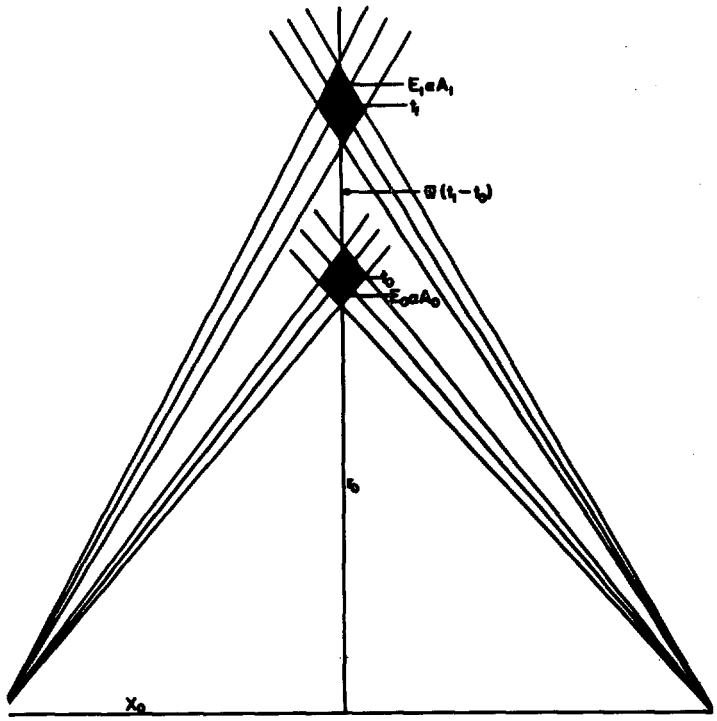

FIGURE 2.—Error areas at times t_0 and t_1, for a true average wind $\overline{W}$, and for a balloon moving normal to the base line.

degrading of angle data through the transmission and digital encoding systems. (4) Reasonable tracking conditions exist, i.e., the base line is of sufficient length, the balloon does not move parallel to the base line, and is not directly above one of the operators.

In light of these assumptions, a specific question must be answered. For what purposes are the wind velocity data to be used? There are several possible uses, such as wind profile studies, space-time wind variability studies, wind shear determinations, ballistics, and low-level jet studies. Depending on the type and mode (real-time versus non-real-time, manual reduction versus computer reduction) of application, it is desirable to use either an average value through a height layer, such as in ballistics, or velocities at specific heights, as in profile or shear studies.

An average, if desired, can be estimated by the equation

$$\overline{W}=\frac{1}{t_1-t_0}\int_{t_0}^{t_1} f'(t)dt=\frac{f(t_1)-f(t_0)}{t_1-t_0} \qquad (1)$$

where $f'(t)$ is the time derivative of a function which describes the space points in the layer, and t_0 and t_1 are the times when the balloon is at the bottom and top of the layer. This implies that regardless of the layer thickness the ability to determine the average is dependent on how well $f(t)$ can be evaluated at the bottom and top of the layer.

In the simplest case (fig. 2), equation (1) for the speed part only can be written

$$\overline{W}^*=\frac{\overline{W}(t_1-t_0)\pm(E_0^2+E_1^2)^{1/2}}{t_1-t_0} \qquad (2)$$

where $\overline{W}^*$ is the computed mean wind speed including precision errors, $\overline{W}$ is the true mean speed for time interval (t_1-t_0) and E_0, E_1 are errors which are assumed to be independent of one another. The effect of errors on direction was not made part of this study.

Let $E \propto \sqrt{A}$, i.e., the error is proportional to the intersection of the horizontal projection of the precision cones (fig. 3), or $E=K\sqrt{A}$ where K is a proportionality constant.

The area, A, can be computed by geometric and trigonometric applications (see fig. 3). A small angle approximation of A (the small angle approximation is applied to the angle B) results in the following formula:

$$A=\frac{4L^2B^2[\sin\psi\,\sin\theta-B^2\cos\psi\,\cos\theta\,\cos^2(\psi+\theta)]}{\sin(\psi+\theta)[\sin^2(\psi+\theta)-4B^2\cos^2(\psi+\theta)]} \qquad (3)$$

where

$$\psi=\cos^{-1}\frac{R^2+L^2-p^2R^2}{2RL},\ \theta=\cos^{-1}\frac{p^2R^2+L^2-R^2}{2pLR},$$

B is half the range of azimuth precision, and p is a factor as shown in figures 3 and 4. This approximation is valid for B small, a reasonable assumption, and when the balloon is not on or very near the base line. In addition, from figure 4,

$$R=[R_0^2+2\overline{W}(t-t_0)\sqrt{R_0^2-X_0^2}\cos\phi$$
$$+\overline{W}^2(t-t_0)^2-2X_0\overline{W}(t-t_0)\sin\phi]^{1/2}$$

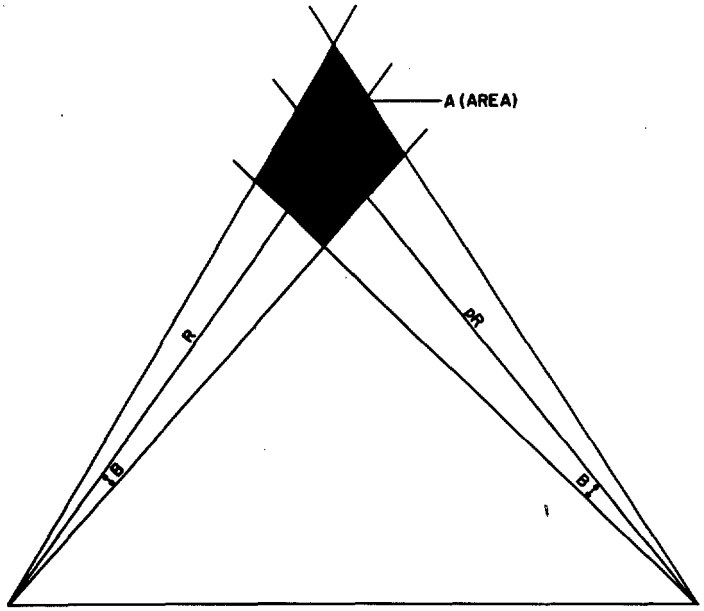

FIGURE 3.—The relationship between error area, precision angle B and range R. Also shown in the graph is the significance of p.

and

$$p=\frac{1}{R}\left[R^2-(X_0-\overline{W}(t-t_0)\sin\phi)^2 + (L-X_0+\overline{W}(t-t_0)\sin\phi)^2\right]^{1/2}. \quad (4)$$

Since $E\propto\sqrt{A}$ and

$$A=\frac{4L^2B^2[\sin\psi\sin\theta-B^2\cos\psi\cos\theta\cos^2(\psi+\theta)]}{\sin(\psi+\theta)[\sin^2(\psi+\theta)-4B^2\cos^2(\psi+\theta)]},$$

then E can be written as

$$E=\frac{2KLB[\sin\psi\sin\theta-B^2\cos\psi\cos\theta\cos^2(\psi+\theta)]^{1/2}}{\{\sin(\psi+\theta)[\sin^2(\psi+\theta)-4B^2\cos^2(\psi+\theta)]\}^{1/2}} \quad (5)$$

where K is the proportionality constant.

In particular, at times t_0 and t_1,

$$E_0=\frac{2KLB[\sin\psi_0\sin\theta_0-B^2\cos\psi_0\cos\theta_0\cos^2(\psi_0+\theta_0)]^{1/2}}{\{\sin(\psi_0+\theta_0)[\sin^2(\psi_0+\theta_0)-4B^2\cos^2(\psi_0+\theta_0)]\}^{1/2}}. \quad (6)$$

and

$$E_1=\frac{2KLB[\sin\psi_1\sin\theta_1-B^2\cos\psi_1\cos\theta_1\cos^2(\psi_1+\theta_1)]^{1/2}}{\{\sin(\psi_1+\theta_1)[\sin^2(\psi_1+\theta_1)-4B^2\cos^2(\psi_1+\theta_1)]\}^{1/2}}. \quad (7)$$

Substituting equations (6) and (7) into (2) results in

$$\overline{W}^*=\overline{W}\pm\frac{2KLB}{(t_1-t_0)}\left\{\frac{\sin\psi_0\sin\theta_0-B^2\cos\psi_0\cos\theta_0\cos^2(\psi_0+\theta_0)}{\sin(\psi_0+\theta_0)[\sin^2(\psi_0+\theta_0)-4B^2\cos^2(\psi_0+\theta_0)]} + \frac{\sin\psi_1\sin\theta_1-B^2\cos\psi_1\cos\theta_1\cos^2(\psi_1+\theta_1)}{\sin(\psi_1+\theta_1)[\sin^2(\psi_1+\theta_1)-4B^2\cos^2(\psi_1+\theta_1)]}\right\}^{1/2}. \quad (8)$$

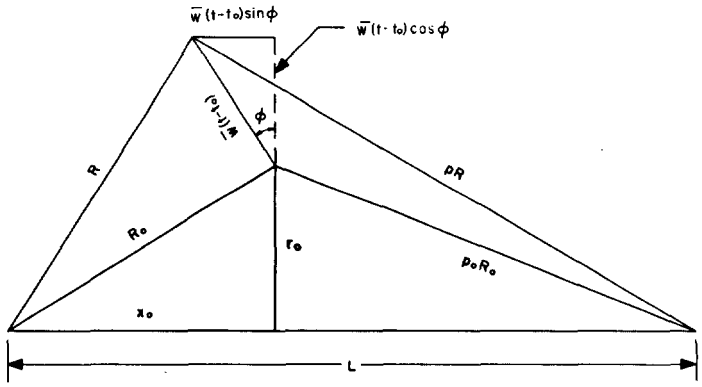

FIGURE 4.—Geometrical representation interrelating the base line L, range R, x_0, R_0, and the average velocity $\overline{W}$ for a balloon moving at the angle ϕ from the normal to the base line.

A graph of the absolute value of $|(\overline{W}^*/\overline{W})-1|$ as a function of (t_1-t_0) for $K=1$ is shown in figure 5 for different values of $\overline{W}$. The value $K=1$ was chosen for convenience in drawing the graphs. It is easy to see that if a different value of K were used, the graphs would still have the same general shape. The most significant feature of the graph is that the error is greater for smaller (t_1-t_0), which is in agreement with Barnett and Clarkson's results. Hence, two independent approaches have shown that the errors in the mean wind computed through a layer tend to be smaller the "longer the observational time interval (i.e. the thicker the layer)."

Up to this point, errors due only to instrument precision have been considered. This can be extended to include the effects of operator errors (tracking) by observing that geometrically only B is affected and will in fact be increased when human tracking error is included. However, B will probably be smaller for larger (t_1-t_0), but not less than the precision alone, since it is more difficult to track and read at a fast rate (strictly a human limitation). Exceptions to these general results occur when gross operator errors are made, and it is this situation which produces "spikes" in the data. These results substantiate the findings of Barnett and Clarkson; however, both studies were based on the simple model—in particular, on the assumption that only one observation point is available at the bottom and top of each layer.

The following discussion shows conclusively that frequent observations through a layer will provide better results than only an observation at the top and bottom of the layer and hence that, except for very thin layers, the results depicted in figures 1 and 4 can be misleading. In addition, it points out the need for minimizing B, which in turn suggests that tracking systems be used which eliminate the operator error (Glass [3]).

A well known theorem from statistics (e.g., Wadsworth and Bryan [5]) will be used to show that, subject to appropriate and reasonable assumptions, the error in the mean wind (expressed in terms of a standard deviation)

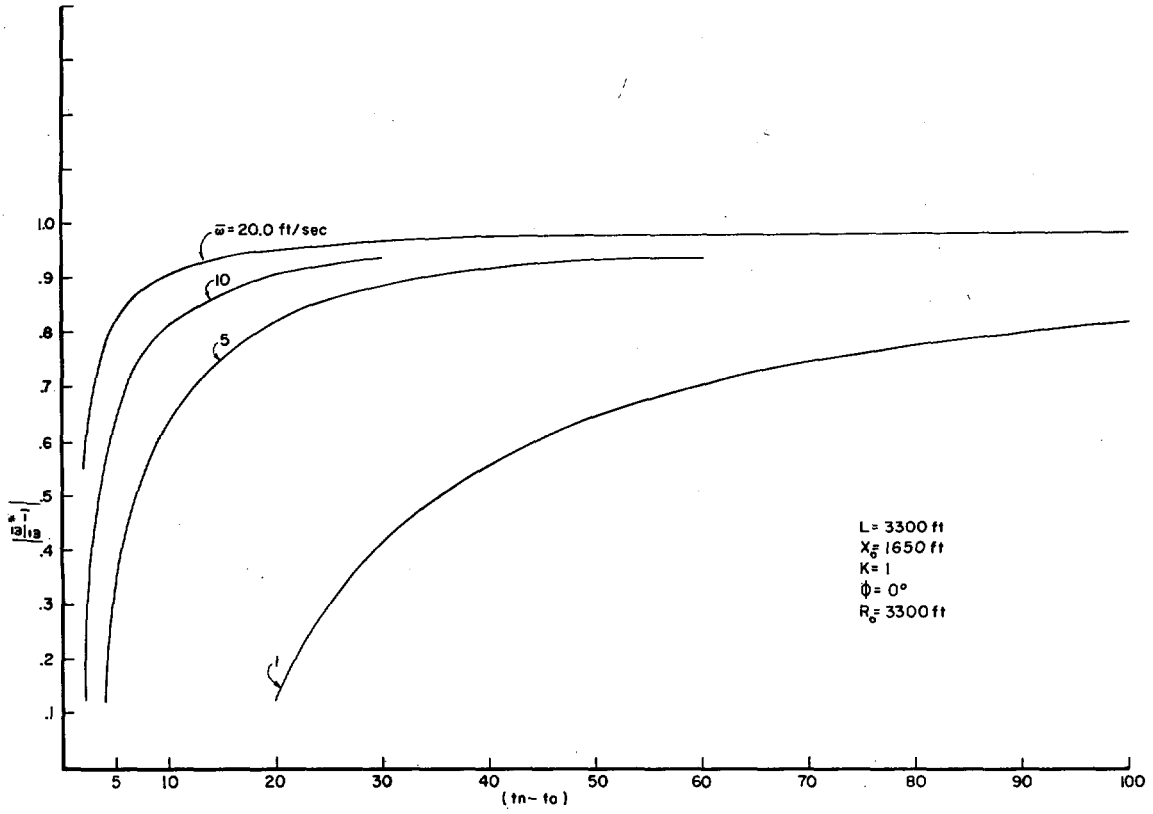

FIGURE 5.—$\left|\frac{\overline{W}^*}{\overline{W}} - 1\right|$ as a function of time interval (sec.) between readings for base line $L=3300$ ft., $x_0=1650$ ft., K (the proportionality constant) $=1.0$, $\phi=0°$, and $R_0=3300$ ft.

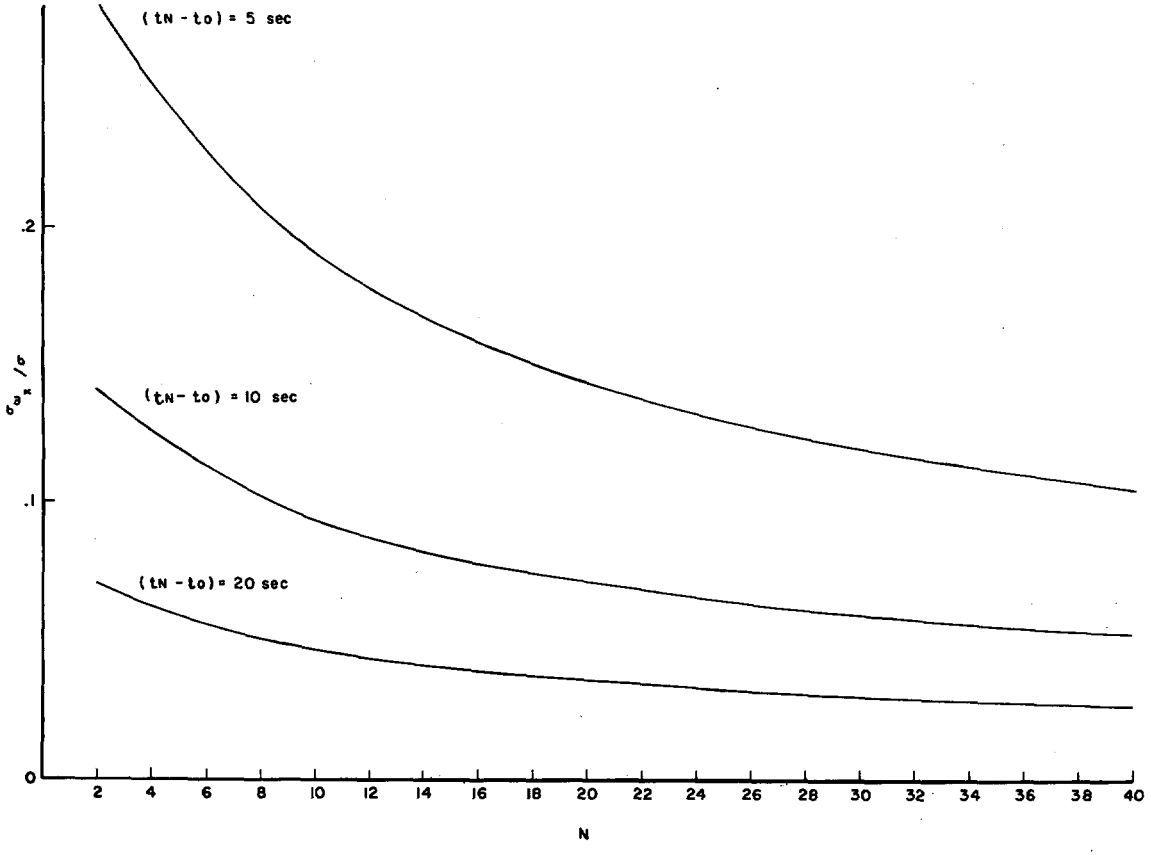

FIGURE 6.—Ratio of σ_{W_x} to σ as a function of N for different values of $(t_n - t_0)$.

decreases as the number of measurements within the layer increases. This theorem is stated below.

Theorem: If $\{X_i\}_{i=1}^N$ are independent, normally distributed random variables with respective parameters $(\mu_1, \sigma_1) \ldots, (\mu_n, \sigma_n)$, and if $\{a_i\}_{i=1}^N$ are constants at least one of which is nonzero, then the weighted sum $X=\Sigma a_i X_i$ is normally distributed with parameters (μ, σ) where

$$\mu=\sum a_i\mu_i \tag{9}$$

and

$$\sigma=\sqrt{\sum a_i^2\sigma_i^2}. \tag{10}$$

In the following analysis it will be assumed that if $\{X_i\}_{i=0}^N$ represents the x-components of the position at times $\{t_0+i\Delta t\}_{i=0}^N$, then the X_i's are independent, normally distributed, random variables homoscedastic with standard deviation σ. To derive an estimate of either W_x or σ_{W_x} it is necessary to make some assumption concerning the function $X=f(t)$. It is usually assumed that $f(t)$ is linear over the time interval $[t_0, t_0+N\Delta t]$. Under this assumption one can write $f(t)=at+b$. Now equation (1) becomes $W_x=a$. Least squares techniques are applied to the pairs $(X_i, t_i)_{i=0}^N$ to determine a $(t_i=t_0+i\Delta t)$. One obtains

$$a=\sum_{i=0}^{N} X_i\left(\frac{\sum t-t_i(N+1)}{(\sum t)^2-(N+1)\sum t^2}\right). \tag{11}$$

W_x is of the form $W_x=\Sigma\, a_i X_i$. Thus the theorem is applicable and σ_{W_x} is

$$\sigma_{W_x}=\sigma\sqrt{\sum_{i=0}^{N}\left[\frac{\Sigma t-t_i(N+1)}{(\Sigma t)^2-(N+1)t^2}\right]^2}. \tag{12}$$

After considerable simplification this becomes

$$\sigma_{W_x}=\frac{\sigma}{t_n-t_0}\sqrt{\frac{12N}{(N+1)(N+2)}} \tag{13}$$

which clearly decreases as N increases and therefore substantiates the marked advantage of faster sampling as shown in figure 6.

Since σ is not known, the ratio σ_{W_x}/σ was plotted as a function of N for different values of t_n-t_0. Note that for $(t_n-t_0)=10$ sec. (which corresponds to a height interval of approximately 170 ft. for a conventional 100-gm. balloon), σ_{W_x}/σ is reduced by approximately 30 percent if one uses 10 points instead of 2; whereas for $(t_n-t_0)=20$ sec., σ_{W_x}/σ is reduced by 50 percent if one uses 20 points instead of 2. Whether these percentage improvements are significant depends on the magnitude of σ, which of course depends on the tracking system being used.

Also, note that σ_{W_x} for $(t_n-t_0)=20$ sec., is always approximately 50 percent of σ_{W_x} for $(t_n-t_0)=10$ sec., so that the effect of (t_n-t_0) in general overrides the effect due to N. Therefore, if one can determine, for instance, that a height layer corresponding to 20 sec. of flight is suitable for an application instead of a 10-sec. layer there is a general improvement of 50 percent from use of the 20-sec. layer. In turn, however, if $N=20$ instead of 2 for the 20-sec. interval there is a further improvement of 50 percent.

Finally, equation (13) does show that σ_{W_x} decreases as t_n-t_0 increases which agrees with Barnett and Clarkson's results for $t_n-t_0\leq 20$ sec. but not with their results for $t>20$. This latter disagreement may be due both to the assumption that $f(t)$ is linear (which was also assumed by Barnett and Clarkson), and to the fact that the assumption of homoscedasticity of the X_i's probably becomes less valid for t_n-t_0 large.

3. CONCLUSIONS

Results of using the two methods for analyzing sampling rate problems substantiate Barnett and Clarkson's findings that the errors in a computed mean wind (using pilot-balloon data) through a layer tend to be smaller the larger the layer.

However, it is also shown, rather conclusively, that many observations through a layer will provide much better average wind estimates than only two, i.e., one at the bottom and one at the top of the layer.

Qualitative analyses of the equations for combined precision and operator errors show that automatic tracking systems should be used for pilot-balloon wind computations.

REFERENCES

1. K. M. Barnett and O. Clarkson, Jr., "Relation of Time Interval to the Accuracy of Double Theodolite Observations," *Monthly Weather Review*, vol. 93, No. 6, June 1965, pp. 377–379.
2. L. D. Duncan and H. Rachele, "Real-Time Meteorological System for Firing of Unguided Rockets," ECOM–5037, Atmospheric Sciences Laboratory, White Sands Missile Range, N. Mex., Feb. 1966.
3. R. I. Glass, Jr., "Rocket Impact Prediction Equipment at White Sands Missile Range," U.S. Army Electronics Research and Development Activity, White Sands Missile Range, N. Mex., Nov. 1964.
4. H. Rachele and L. D. Duncan, "Prelaunch Real-Time Impact Prediction System and Research Program for the Athena Rocket," U.S. Army Electronics Research and Development Activity, White Sands Missile Range, N. Mex., Nov. 1964.
5. G. P. Wadsworth and J. G. Bryan, *Introduction to Probability and Random Variables*, McGraw-Hill Book Co., Inc., New York, 1960.

[*Received August 31, 1966; revised January 9, 1967*]